Simulation and Verification of 3D Printed Oscillators for Vibration Energy Harvester

Philipp Gawron[1], Thomas M. Wendt[1], Nikolai Hangst[1], Lukas Stiglmeier[1], Urban B. Himmelsbach[1], and Anke Fischer[1]
[1]Offenburg University of Applied Sciences, Work-Life Robotics Institute, Offenburg, Germany

Abstract

3D printing offers customisation capabilities regarding suspensions for oscillators of vibration energy harvesters. Adjusting printing parameters or geometry allows to influence dynamic properties like resonance frequency or bandwidth of the oscillator. This paper presents simulation results and measurements for a spiral shaped suspension printed with polylactic acid (PLA) and different layer heights. Eigenfrequencies have been simulated and measured and damping ratios have been experimentally determined.

1 Introduction

Utilising 3D printing to create vibration energy harvesters offers customisation capabilities regarding the suspension's geometry. Adjusting the resonance frequency or bandwidth of the harvester would allow to optimise the device for each application. Mechanical energy in general can be harvested via electromagnetic [1, 2], electrostatic [3] or piezoelectric [4] harvesting techniques. Photovoltaic cells convert solar energy into electrical energy [5]. Thermoelectric generators (TEG) convert thermal into electrical energy [6]. Radiofrequency (RF) harvesting harvest ambient RF sources, for example television signal or mobile phone stations [7].

Compared to traditional technologies such as moulding 3D printing offers benefits like faster development, no requirement of moulds, fewer additional process steps for fabrication of complex geometries as well as potential of waste-, lead time- and cost-reduction [8, 9]. A review of 3D printed electromagnetic vibration energy harvesters has been conducted in [10]. Mentioned benefits for printed harvesting devices are multi-material-printing, utilisation of functional materials, monolithic fabrication as well as miniaturisation capabilities with certain printing processes like inkjet. The fabrication of complex structures offers a fast and easy way to create variations of suspensions for vibration energy harvesters.

In [11] various inkjet-printed suspensions have been investigated regarding their eigenfrequency (also known as natural frequency). In [12] different suspensions printed with acrylonitrile butadiene styrene (ABS) via fused filament fabrication (FFF) have been experimentally investigated. Both studies have shown that printed suspensions are viable for energy harvesting and that changing the suspension's parameters or geometry allows to influence the harvester's resonance frequency. Mechanical damping has not been investigated in both studies. In order to estimate for example the bandwidth of a harvester via simulation the damping is necessary. Therefore, this paper researches the damping of a FFF printed spiral shaped suspension made of PLA.

2 Methods and Materials

For this research an isotropic material was utilised based on the values in [13]. The material PLA with a Poisson's ratio of 0.37 was applied along with a specific gravity of 1.24 g cm^{-3}. The modulus of elasticity was exchanged for the one of the utilised printing material (Prusament PLA Galaxy Black [14]) with 2200 MPa. Damping been neglected for the eigenfrequency simulation since a low damping ratio is expected. For example a damping ratio of $\zeta = 0.1$ leads to difference of 0.5% between the damped eigen angular frequency ω_D and the undamped, natural eigen angular frequency ω [15]. The investigated suspension shape is shown in **Fig. 1** and the geometric and printing parameters in **Tab. 1**.

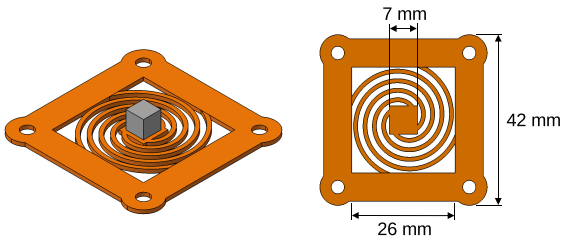

Figure 1 Suspension with spiral shape, (left) isometric view with magnets on top and bottom, (right) top view without magnets

The specimen were 3D printed on a Neotech AMT 15X SA with 0.2 mm and 0.1 mm layer height. NdFeB N50 magnets (5 mm × 5 mm × 5 mm) were utilised as seismic mass. For simulation the material BMN-50 from the COMSOL library with a density of 7.55 g cm^{-3} was applied for the magnets. The measured height of the printed specimen was 1.1 mm which was utilised for the simulation.

ISBN 978-3-8007-5835-7

Table 1 Geometric and printing parameters

Parameter	Value
Outer edge length	42 mm
Inner edge length	26 mm
Platform	7 mm × 7 mm
Width spiral arm	1 mm
Height	1.1 mm
Nozzle diameter	0.4 mm
Layer height	0.1 mm, 0.2 mm
Infill	100%
Printing pattern	Rectilinear
Raster angle	45°

2.1 Theory

Free vibration was initiated to the printed suspension by a shaker (YMC MS-20). The induced motion was recorded with a laser vibrometer (OptoMET Dual Sense I) and evaluated in MATLAB. The logarithmic decrement-method was then utilised to determine the eigenfrequency and damping ratio [15, 16]. The logarithmic decrement δ can be calculated with (1)

$$\delta = \frac{1}{n} ln \frac{x_i}{x_{i+n}} \tag{1}$$

where x_i and x_{i+n} are consecutive peaks in the recorded signal. Then the damping ratio ζ_{LogDec} can be calculated with (2).

$$\zeta_{LogDec} = \frac{\delta}{\sqrt{(2\pi)^2 + \delta^2}} \tag{2}$$

From the measured signal the period T_D can be determined. Then the damped eigen angular frequency ω_D can be calculated with (3)

$$\omega_D = \frac{2\pi}{T_D} \tag{3}$$

and the damped eigenfrequency f_D with (4).

$$f_D = \frac{\omega_D}{2\pi} \tag{4}$$

Additionally curve fitting of an exponential function (5)

$$u(t) = ae^{-bt} \tag{5}$$

to the measured signal's peaks was applied as a second method to determine ζ. With the determined eigen angular frequency ω_D and the coefficient b, $\zeta_{Curvefit}$ can then be calculated with (6).

$$\zeta_{Curvefit} = \frac{b}{\omega_D} \tag{6}$$

2.2 Measurement Setup

Fig. 2 shows the measurement setup consisting of a shaker with a needle attached to it and the mounted suspension with magnets. The suspension's frame was clamped by a printed mounting. A laser vibrometer was arranged above. A pulse signal was applied to the shaker in order to cause an up- and down movement of the needle. This resulted in an initial displacement of the suspension-magnet-combination and thus induced free vibration.

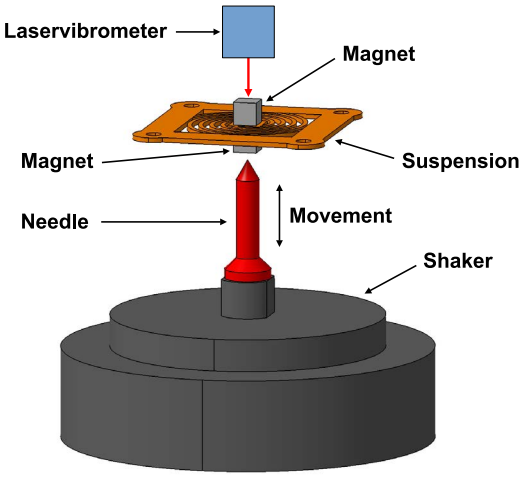

Figure 2 Measurement setup to initiate and record free vibration

3 Results

The free vibration response of a suspension after triggering by the shaker's needle is shown in **Fig. 3**. The initial displacement in this case was around 330 µm. After identifying the signal's peaks the period T_D and the logarithmic decrement δ were determined. The simulation and measurement results for the eigenfrequency are shown in **Tab. 2**. The measured eigenfrequencies were between 35.75 to 37.37 Hz depending on the applied layer height while the simulated eigenfrequency was 36.01 Hz. **Tab. 3** shows the results of four series of measurements with the initial displacement caused by the shaker, the damped eigenfrequency f_D and both calculation results for the damping ratios ζ_{LogDec} and $\zeta_{Curvefit}$.

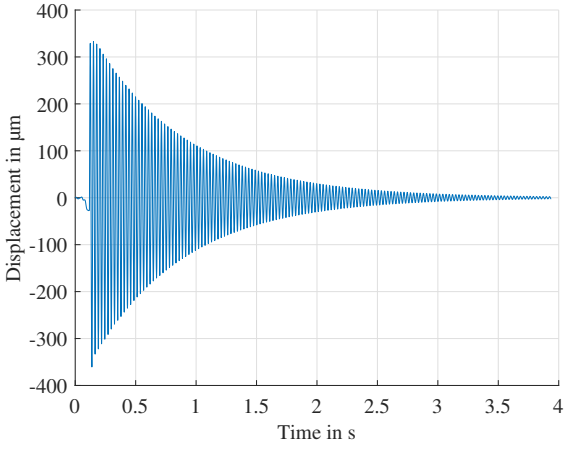

Figure 3 Measured response of the suspension after initial displacement

Table 2 Results for the first eigenfrequency of the suspensions

Source	Layer Height	**Value**
Simulation	-	36.01 Hz
Suspension 1	0.2 mm	35.75±0.01 Hz
Suspension 1	0.2 mm	35.77±0.01 Hz
Suspension 2	0.2 mm	35.40±0.01 Hz
Suspension 3	0.1 mm	37.37±0.01 Hz

4 Discussion

The measured eigenfrequencies during the 25 cycles of each suspension were 35.75±0.01 Hz, 35.77±0.01 Hz, 35.40±0.01 Hz and 37.37±0.01 Hz as shown in Tab. 2. A standard deviation of ±0.01 Hz shows the good consistency regarding the eigenfrequencies. The difference between suspension 1 (35.75±0.01 Hz) and 2 (35.40±0.01 Hz) was 0.1% which indicates consistent eigenfrequencies for identically printed suspensions. The simulated eigenfrequency of 36.01 Hz correlates well with the measured eigenfrequencies. It is notable that suspension 3 showed a higher eigenfrequency. The smaller layer height of 0.1 mm could increase the stiffness of the suspension and thus increase the eigenfrequency. The authors in [19] investigated the effect of printing parameters on the tensile properties of PLA printed test specimen. It was reported that the infill density had the highest contribution towards the Young's modulus while layer height was less significant. Considering the investigated suspensions in this paper no actual infill pattern was utilised. The parallel printing traces of the spiral arms were located right next to each other leading to nearly 100% infill density. A reduction in layer height might decrease the air gaps between the traces of each layer and thus influence the suspension's properties.

Tab. 3 shows the initial displacement, the eigenfrequency f_D and the damping ratios ζ_{LogDec} and $\zeta_{Curvefit}$. Due to the shaker's characteristic the initial displacement was measured with the laser vibrometer. The damping ratios ζ for all tested suspensions ranged between 5.18×10^{-3} to 5.56×10^{-3}. Both methods to calculate ζ_{LogDec} and $\zeta_{Curvefit}$ showed similar results. Occurring transient effects at the beginning have been neglected, because they would affect the damping ratio's calculation. The first measurement series of suspension 1 showed such a transient effect where the very first peak had a displacement around 450 µm due to the shaker's characteristic. The following two peaks of the response then dropped to around 200 µm, where the free vibration started. Without neglecting the first peak the resulting damping ratio would be 5.90×10^{-3}. By neglecting the first peak the damping ratio was calculated with 5.23×10^{-3}. A second measurement of suspension 1 was done (without occurring transient effect) resulting in a damping ratio of 5.18×10^{-3}. These values match well with suspension 2 and 3. Over all the damping ratios of all three suspensions are close to each other, indicating a good repeatability of the printing process. Systems with $\zeta < 1$ are considered under damped [17]. They can effectively harvest energy, but have a narrow bandwidth [18]. Thus, these suspensions could harvest with a narrow bandwidth. Or to increase the bandwidth the damping ratio would have to be increased, either by adapting geometric parameters, shape or by utilising another material for the suspensions.

5 Conclusion

3D printed suspensions offer customisation with various parameters to tune the suspension's properties. The investigated spiral-shape with different layer heights showed eigenfrequencies between 35 to 37 Hz. The measured damping ratios of the under damped systems ranged between 5.18×10^{-3} to 5.56×10^{-3}. It has been showed, that 3D printed suspensions can achieve low damping ratios and thus can be utilised to create energy harvesters with a narrow bandwidth.

6 Future Work

The effects of geometry, other materials than PLA as well as printing parameters like layer height, infill pattern or nozzle diameter on the properties of 3D printed suspensions will be subject of future research.

7 Acknowledgement

Funded by the Deutsche Forschungsgemeinschaft (DFG, German Research Foundation) – 426605889.

8 Literature

[1] L. Wang, P. Todaria, A. Pandey, J. O'Connor, B. Chernow, and L. Zuo, "An Electromagnetic Speed Bump Energy Harvester and Its Interactions With Vehicles," IEEE/ASME Trans. Mechatron., vol. 21, no. 4, pp. 1985–1994, 2016, doi: 10.1109/TMECH.2016.2546179.

[2] T. Wendt, P. Gawron, and L. Stiglmeier, "Kinetic Energy Harvesting in a driven Tool Holder," in Proceedings MikroSystemTechnik Kongress 2021, Berlin: VDE Verlag GmbH, 2021, pp. 684–687.

[3] R. T. Aljadiri, L. Y. Taha, and P. Ivey, "Electrostatic Energy Harvesting Systems: A Better Understanding of Their Sustainability," JOCET, vol. 5, no. 5, pp. 409–416, 2017, doi: 10.18178/JOCET.2017.5.5.407.

[4] J. Zhao and Z. You, "A shoe-embedded piezoelectric energy harvester for wearable sensors," Sensors (Basel, Switzerland), vol. 14, no. 7, pp. 12497–12510, 2014, doi: 10.3390/s140712497.

[5] M.-L. Ku, W. Li, Y. Chen, and K. J. Ray Liu, "Advances in Energy Harvesting Communications: Past, Present, and Future Challenges," IEEE Commun.

Table 3 Values for eigenfrequency f_D and damping ratio ζ with n=25 for the three suspensions

Parameter	Statistical value	Suspension 1		Suspension 2	Suspension 3
Layer height		0.2 mm		0.2 mm	0.1 mm
Initial displacement in µm	$\bar{x}$	203.88	279.67	360.22	341.13
	σ	9.19	5.23	5.17	6.34
	Min	198.73	271.92	352.88	330.24
	Max	246.18	288.29	369.64	354.75
f_D in Hz	$\bar{x}$	35.75	35.77	35.40	37.37
	σ	13.04×10^{-3}	12.77×10^{-3}	13.29×10^{-3}	10.04×10^{-3}
	Min	35.69	35.71	35.33	37.33
	Max	35.76	35.78	35.41	37.38
ζ_{LogDec}	$\bar{x}$	5.23×10^{-3}	5.18×10^{-3}	5.24×10^{-3}	5.54×10^{-3}
	σ	5.24×10^{-5}	6.94×10^{-5}	4.47×10^{-5}	5.90×10^{-5}
	Min	5.13×10^{-3}	5.08×10^{-3}	5.19×10^{-3}	5.41×10^{-3}
	Max	5.36×10^{-3}	5.46×10^{-3}	5.41×10^{-3}	5.74×10^{-3}
$\zeta_{Curvefit}$	$\bar{x}$	5.26×10^{-3}	5.22×10^{-3}	5.26×10^{-3}	5.56×10^{-3}
	σ	8.23×10^{-5}	8.45×10^{-5}	3.94×10^{-6}	4.65×10^{-6}
	Min	5.22×10^{-3}	5.20×10^{-3}	5.25×10^{-3}	5.56×10^{-3}
	Max	5.70×10^{-3}	5.63×10^{-3}	5.27×10^{-3}	5.58×10^{-3}

Surv. Tutorials, vol. 18, no. 2, pp. 1384–1412, 2016, doi: 10.1109/COMST.2015.2497324.

[6] G. Verma and V. Sharma, "A Novel Thermoelectric energy harvester for Wireless Sensor Network Application," IEEE Trans. Ind. Electron., pp. 3530–3538, 2019, doi: 10.1109/TIE.2018.2863190.

[7] M. Pinuela, P. D. Mitcheson, and S. Lucyszyn, "Ambient RF Energy Harvesting in Urban and Semi-Urban Environments," IEEE Trans. Microwave Theory Techn., vol. 61, no. 7, pp. 2715–2726, 2013, doi: 10.1109/TMTT.2013.2262687.

[8] I. Gibson, D. Rosen, B. Stucker, and M. Khorasani, Additive Manufacturing Technologies, 3rd ed. Cham: Springer, 2021.

[9] F. Calignano et al., "Overview on Additive Manufacturing Technologies," Proc. IEEE, vol. 105, no. 4, pp. 593–612, 2017, doi: 10.1109/JPROC.2016.2625098.

[10] P. Gawron, T. M. Wendt, L. Stiglmeier, N. Hangst, and U. B. Himmelsbach, "A Review on Kinetic Energy Harvesting with Focus on 3D Printed Electromagnetic Vibration Harvesters," Energies, vol. 14, no. 21, p. 6961, 2021, doi: 10.3390/en14216961.

[11] B. Kawa, K. Śliwa, V. C. Lee, Q. Shi, and R. Walczak, "Inkjet 3D Printed MEMS Vibrational Electromagnetic Energy Harvester," Energies, vol. 13, no. 11, p. 2800, 2020, doi: 10.3390/en13112800.

[12] P. Garcia-Moreno, M. E. Perez, F. J. Estevez, and P. Gloesekoetter, "Study of Wearable and 3D-Printable Vibration-Based Energy Harvesters," in 2016 15th International Conference on Ubiquitous Computing and Communications and 2016 International Symposium on Cyberspace and Security (IUCC-CSS), Granada, Spain, 2016, pp. 101–108.

[13] M.-M. Pastor-Artigues, F. Roure-Fernández, X. Ayneto-Gubert, J. Bonada-Bo, E. Pérez-Guindal, and I. Buj-Corral, "Elastic Asymmetry of PLA Material in FDM-Printed Parts: Considerations Concerning Experimental Characterisation for Use in Numerical Simulations," Materials (Basel, Switzerland), vol. 13, no. 1, 2019, doi: 10.3390/ma13010015.

[14] Prusa Research s.r.o., "Technical Data Sheet Prusament PLA," 2018. Accessed: Mar. 9 2022. [Online]. Available: https://www.prusa3d.com/file/8/technical-data-sheet.pdf

[15] M. Paz and Y. H. Kim, Structural Dynamics. Cham: Springer International Publishing, 2019.

[16] Q. C. Nguyen and H. Q. T. Ngo, "INPUT SHAPING CONTROL TO REDUCE RESIDUAL VIBRATION OF A FLEXIBLE BEAM," JCC, vol. 32, no. 1, pp. 75–90, 2016, doi: 10.15625/1813-9663/32/1/6765.

[17] M. A. Halim, H. Cho, and J. Y. Park, "Design and experiment of a human-limb driven, frequency up-converted electromagnetic energy harvester," Energy Conversion and Management, vol. 106, pp. 393–404, 2015, doi: 10.1016/j.enconman.2015.09.065.

[18] Z. Hadas, C. Ondrusek, and V. Singule, "Power sensitivity of vibration energy harvester," Microsyst Technol, vol. 16, no. 5, pp. 691–702, 2010, doi: 10.1007/s00542-010-1046-4.

[19] L. Auffray, P.-A. Gouge, and L. Hattali, "Design of experiment analysis on tensile properties of PLA samples produced by fused filament fabrication," Int J Adv Manuf Technol, vol. 118, 11-12, pp. 4123–4137, 2022, doi: 10.1007/s00170-021-08216-7.